

ANALYSIS OF A MICROREACTOR FOR SYNTHESIZING NANOCRYSTALS BY COMPUTATIONAL FLUID DYNAMICS

José Carlos Gonçalves Peres¹, Cristhiano da Costa Herrera², Wagner de Rossi², Ardson dos Santos Vianna Jr¹.

¹*University of São Paulo, Polytechnic School, Department of Chemical Engineering*

²*Instituto de Pesquisas Energéticas e Nucleares, Centro de Lasers e Aplicações*

Correspondence: ardson@usp.br

ABSTRACT

A microreactor designed to synthesize nanocrystals was built applying laser pulses with duration of femtoseconds in a quartz board. This precise machining technology allowed dimensioning the microchip cross section as a trapezoidal shape with base lengths of 120 μm and 200 μm and depth of 150 μm . The microchip is comprised of four inlets for reactants, a mixing section with 40 curves after the inlet section to ensure proper mixing of the species and 22 serpentine channels, with 22,000 μm length each, to allow crystal growth.

Flow field throughout the microchip was investigated by computational fluid dynamics considering inlet flow rates between 12.5 and 2000 $\mu\text{L min}^{-1}$. Hexahedral meshes were used to discretize the geometry as its cross section is uniform and to reduce the total number of elements. Advection terms were solved by the high resolution scheme. Numerical solutions were converged when the maximum residual value was less than 10^{-4} and the domain imbalance was less than 1%.

Flow throughout the channels is laminar as the maximum Reynolds number observed is 850. The tridimensional velocity profile is a paraboloid whose vertex is influence by the centrifugal force: at the curved sections, such force accelerates flow towards the outer part of the channels, moving the maximum velocity point to this zone. The centrifugal force also creates secondary flows. These structures enhance mixing in the direction perpendicular to the main flow and behave like turbulent flows in macroscopic systems, allowing proper mixing without additional power consumption.

Proper coupling between microchip geometry and its operating conditions was verified by simulating the dispersion of a non-reactive tracer injected in one of the inlet ports while feeding the others with water. For low flow rates, the tracer flows parallel to the water stream up to half of the mixing section and full mixing occurs after the second serpentine channel. For flow rates higher than 250 $\mu\text{L min}^{-1}$, it shows secondary fluxes are intensified and promote mixing after both the third curve at the mixing section and at the beginning of the serpentine channels after the fourth reactant inlet, ensuring better conditions if the desired reaction is limited by contact between the reactants.

1. INTRODUCTION

Processing with ultrashort laser pulses is a new technology, still in fundamental studies and technological developments, with very different characteristics from any other processing method for material removal.

Because the pulse length of this type of laser is shorter than the electron phonon interaction, one can obtain a process without thermal effects and a machining tool with a diameter less than 1 micron. This tool is thus able to produce structures impossible to obtain with any other method. In addition to tiny structures processed directly on the surface of any type of material, it is also possible processing inside the bulk of transparent materials. Due to extremely high intensities obtained by ultrashort pulses, it is also possible to change the tribological, chemical and physical properties of surfaces. These properties open up new possibilities for processing, with results that are revolutionizing many branches of knowledge..

This precise machining technology allowed dimensioning the microchip cross section as a trapezoidal shape with base lengths of 120 μm and 200 μm and depth of 150 μm .

Flow field throughout the microchip was investigated by computational fluid dynamics considering inlet flow rates between 12.5 and 2000 $\mu\text{L min}^{-1}$. The tridimensional velocity profile is a paraboloid whose vertex is influence by the centrifugal force. Proper coupling between microchip geometry and its operating conditions was verified by simulating the dispersion of a non-reactive tracer injected in one of the inlet ports while feeding the others with water.

2. METHOD

The reactor section is in the Fig. 1. The microchip is comprised of four inlets for reactants, a mixing section with 40 curves after the inlet section to ensure proper mixing of the species and 22 serpentine channels, with 22,000 μm length each, to allow crystal growth.

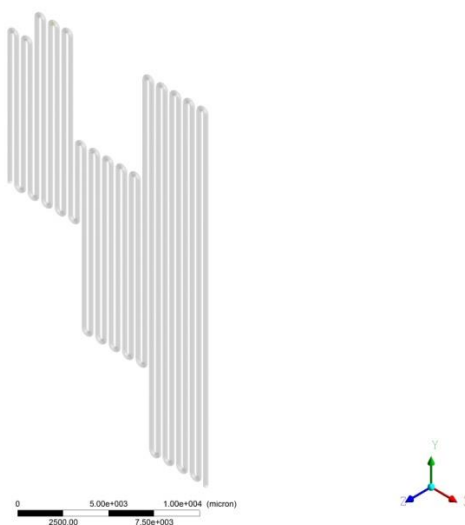


Figure 1 – Isometric vision of analyzed microdispositive

The velocity fields were obtained from operational conditions that are presented in Table 1. This table shows two dimensionless numbers, Reynolds and Dean numbers, which are relevant to the present analysis:

$$\text{Re} = \frac{\bar{u} D}{\eta} \quad (1)$$

$$\text{Dn} = \text{Re} \sqrt{\frac{L}{R_c}} \quad (2)$$

The Dean number can be seen as a balance between inertial forces and centripetal forces.

As the Reynolds number corresponding to the greatest rate flow (Q) were 150, the flow was assumed as laminar. The Navier-Stokes equation in the steady state is:

$$u_j \frac{\partial u_i}{\partial x_j} = -\frac{1}{r} \frac{\partial p}{\partial x_i} + \eta \frac{\partial^2 u_i}{\partial x_j^2} \quad (3)$$

this was numerically solved by finite volume method based on elements. The entrance of the domain was defined from the feed conditions, assuming a plug flow distribution. The boundary condition in the exit was assumed as atmospheric pressure discharge.

Tabel 1 – Operational conditions and dimensionless numbers.

Q ($\mu\text{L min}^{-1}$)	Re	Dn
12,5	0,941	0,043
25	1,88	0,085
50	3,76	0,17
Q ($\mu\text{L min}^{-1}$)	Re	Dn

125	9,41	0,42
250	18,8	0,85
500	37,6	1,7
1000	75,3	3,4
2000	150	6,8

The model was discretised with a hexahedral mesh (Figure 2). The convergence mesh analysis was developed to the curve between 6th and 7th channels (up flow) and to the curve between 11th and 12th channels (down flow), and the rate flow equals to 2000 uL min^{-1} .

(a)

(b)

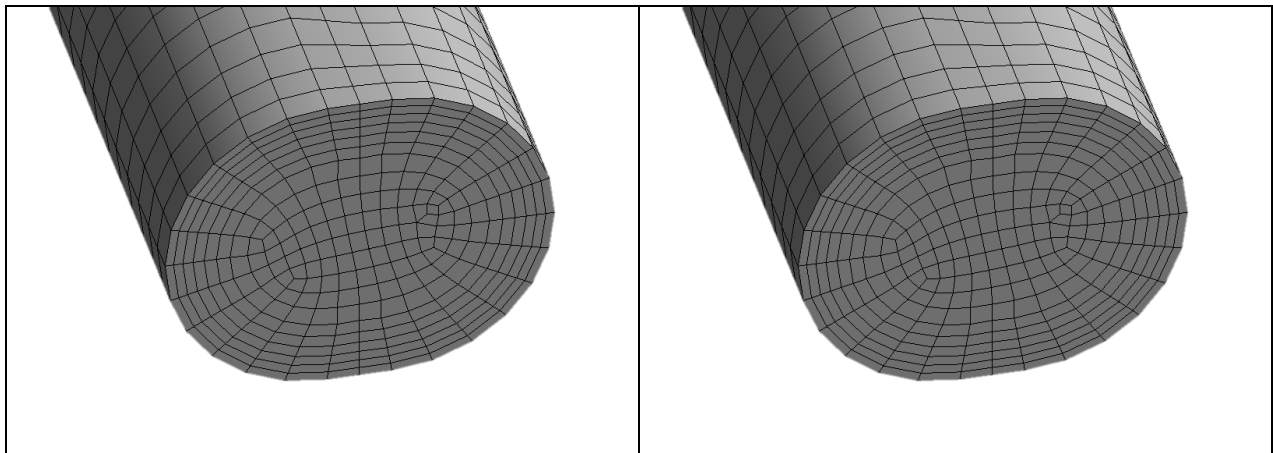


Figure 2 – Two meshes used in CFD simulations: (a) coarse and (b) refine mesh

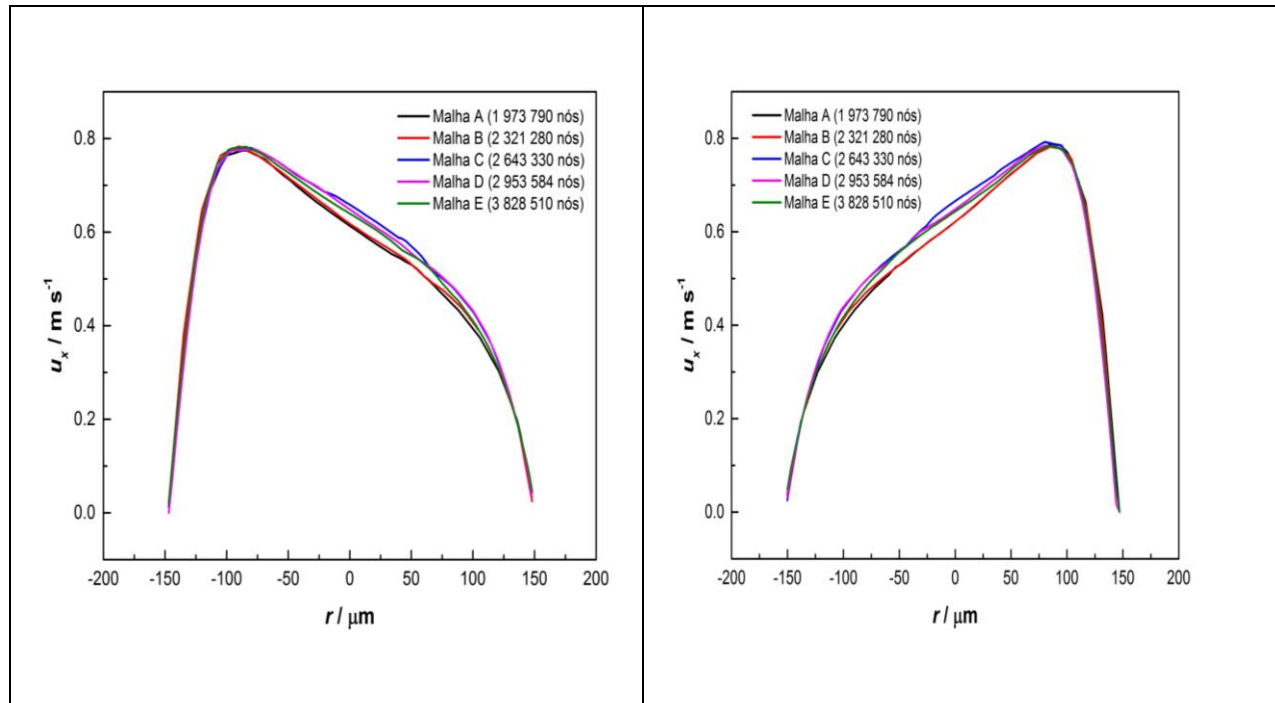


Figure 3 – Mesh analysis – velocity distributions (a) in the curve between 6th and 7th channels (up flow) e (b) in the curve between 11th and 12th channels (down flow).

3. RESULTS

The simulations of microchannel fluid flow make it possible to observe microfluidic phenomena, which are relevant to applications that demand good mixing. The velocity profiles and streamlines can help to understand better the flow that was developed from feed flow and its geometry.

3.1. Velocity profiles

The flow in microchannels was laminar. On the straight section of the tube, the velocity profiles were parabolic, that can be seen in the Figure 4. Despite the system had reduced dimensions, the velocity allowed values of 1 m s^{-1} . The centrifugal force interferes with the velocity distribution: in the curves, the fluid accelerates towards the outside of the channels, shifting the point of maximum speed in this direction:.

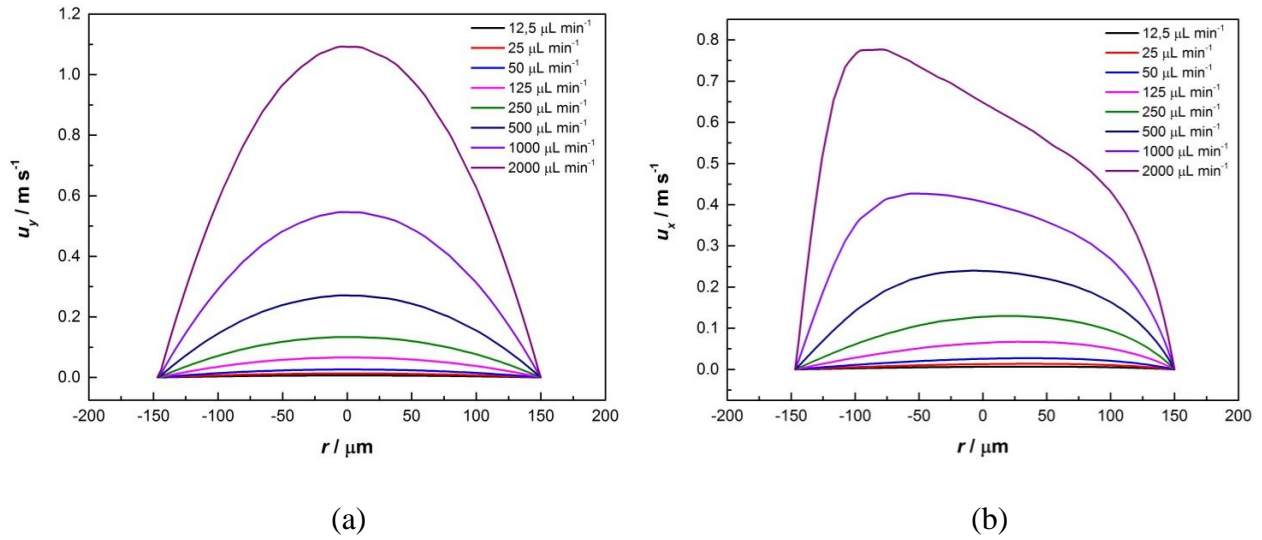


Figure 4 – Effect of flow rate on the velocity field (a) straight section of the tube e (b) in the curve between 6th and 7th channels (up flow)

Another effect of the centrifugal force is the formation of secondary flows in the curve sections. The interaction between the centrifugal forces and the viscous ones cause the formation of a double vortex, which is presented in the Figure 5. The Figure 5(a) shows the vortex in the curve between 6th and 7th channels (up flow), rate flow equal 12,5 $\mu\text{L min}^{-1}$: it can be observed that there was not secondary flow before the curve. This is the Dean Flow, which is characterized by its dimensionless number (Equation 2). If $Dn < 140$, the double vortex will be formed in the curves (Kockmann, 2008), which was observed in the present study.

The secondary flows make mixing better in the microchannels, since they improve diffusive fluxes. It is worth highlighting the vortex was not result of turbulent flows, though it was a secondary flow. The secondary flow are as effective as turbulent flow to improve the mixing process (Kockman, 2008; Kumar *et al.*, 2011).

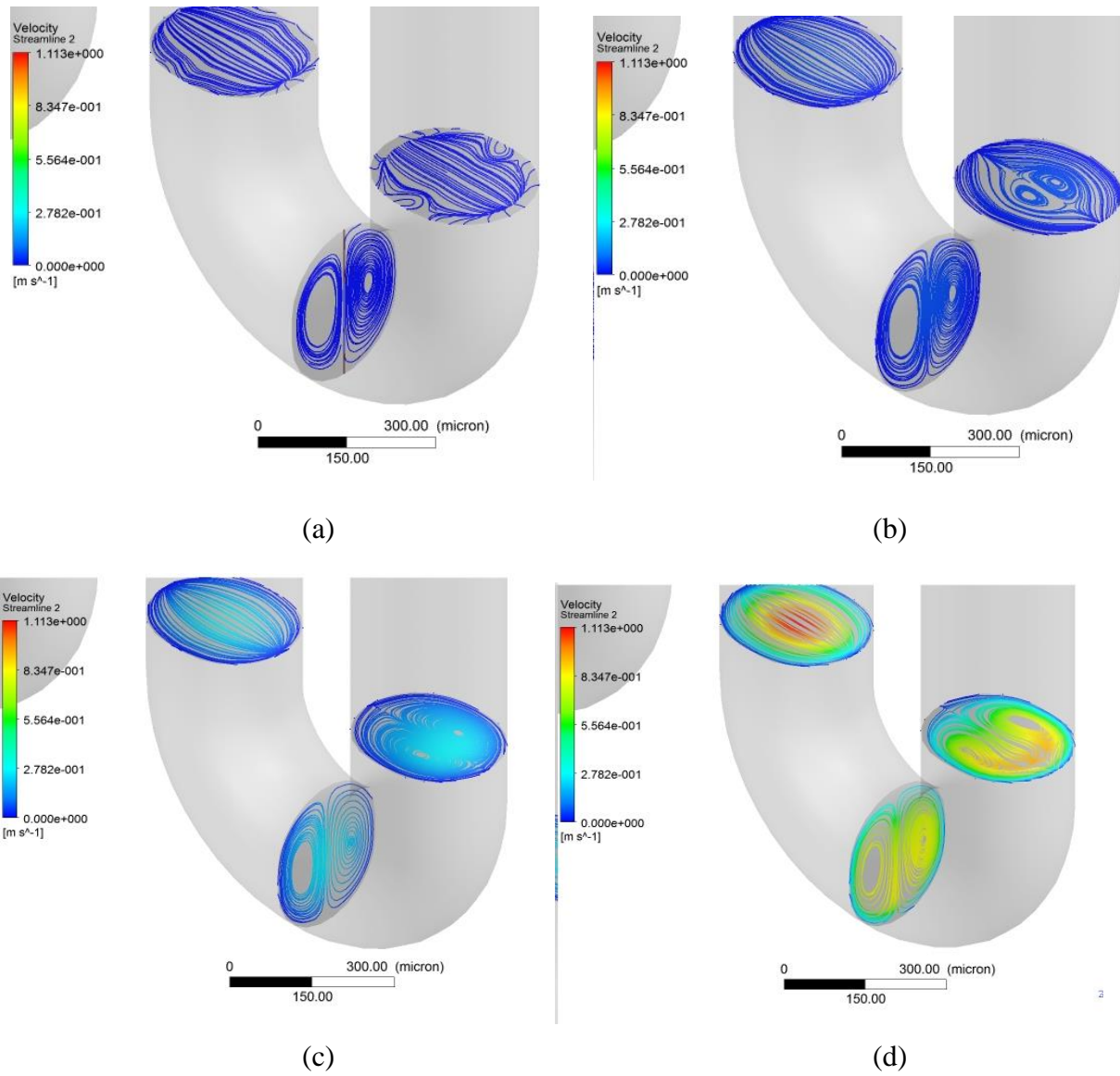


Figure 5– Secondary flows formed in the curve between 6th and 7th channels for rate flows : 12,5; (b) 125; (c) 500 e (d) 2000 $\mu\text{L min}^{-1}$.

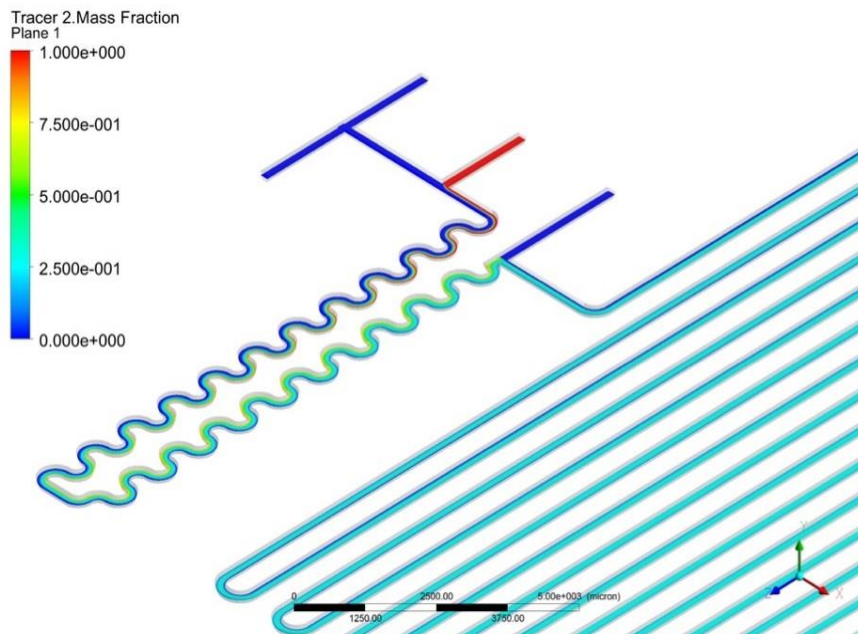


Figure 6 – Impact of the secondary flows on mixing throughout the microchip for inlet flow rates of $12.5 \mu\text{L min}^{-1}$ at the three first inlets.

4. CONCLUSIONS

- The tridimensional velocity profile is a paraboloid whose vertex is influence by the centrifugal force: at the curved sections, such force accelerates flow towards the outer part of the channels,
- Proper coupling between microchip geometry and its operating conditions was verified by simulating the dispersion of a non-reactive tracer injected in one of the inlet ports while feeding the others with water. For low flow rates, the tracer flows parallel to the water stream up to half of the mixing section and full mixing occurs after the second serpentine channel. For flow rates higher than $250 \mu\text{L min}^{-1}$, Figure B shows secondary fluxes are intensified and promote mixing after both the third curve at the mixing section and at the beginning of the serpentine channels after the fourth reactant inlet, ensuring better conditions if the desired reaction is limited by contact between the reactants..

Acknowledgment

This work was supported by São Paulo Research Foundation (FAPESP), grants 2017/19134-8 and 2013/26113-6.



KOCKMANN, N. *Transport Phenomena in Micro Process Engineering*. Berlin: Springer-Verlag, 2008.

KUMAR, V.; PARASCHIVOIU, M.; NIGAM, K. D. P. Single-phase fluid flow and mixing in microchannels. *Chem. Eng. Sci.*, v. 66, p. 1329-1373, 2011.